Phobos proximity orbital transfer analysis with applications to MMX mission

By Nishanth PUSHPARAJ,[1)] Nicola BARESI[2)] and Yasuhiro KAWAKATSU[3)]

[1)] *Department of Space and Astronautical Science, The Graduate University for Advanced Studies,SOKENDAI, Sagamihara, Japan*

[2)] *Surrey Space Centre, University of Surrey, UK*

[3)] *Institute of Space and Astronautical Science, JAXA, Sagamihara, Japan*

(Received November 30th, 2021)

Quasi-satellite orbits (QSOs) are stable retrograde orbits in the restricted three-body problem that have gained attention as a viable candidate for future deep-space missions towards remote planetary satellites. JAXA's robotic sample return mission MMX will utilize QSOs to perform scientific observations of the Martian moon Phobos before landing on its surface and attempt sample retrieval. The complex dynamical environment around Phobos makes the proximity operations of MMX immensely challenging and requires novel and sophisticated techniques for maintaining and transferring between different quasi-satellite orbits. The present paper explores the bifurcated families of QSOs around Phobos for the proximity operations by leveraging dynamical systems theory and using invariant manifolds of unstable retrograde orbits to design transfer trajectories around Phobos. Starting from the equations of the Circular Hill Problem with ellipsoidal Phobos, we first compute families of bifurcated QSOs using in-plane and out-of-plane bifurcations near planar orbits. Through bifurcated families of QSOs, we introduce two novel transfer strategies in the vicinity of Phobos. Later on, the feasibility of using unstable family members as staging orbits between high- and low-altitude QSOs is evaluated. The final candidates are ranked based on MMX scientific requirements, transfer analyses, and station-keeping costs. It is found that intermediate 3D-QSOs can be maintained with as little as 1 m/s per month. Furthermore, it is discovered that transfer from high-altitude QSOs to low-altitude QSOs can be executed with a total ΔV of less than 40 m/s and the total time of flight of less than 5 days.

Key Words: QSOs, 3D-QSOs, Tri-axial Ellipsoid, Orbital Transfers, Hill Problem

1. Introduction

Deep space missions towards remote planetary satellites such as the Martian moons Phobos and Deimos can provide scientists with invaluable clues on the birth and evolution of our solar system. Exploring the Martian moons would shed light on the formation of these satellites, thereby answering whether Phobos and Deimos are captured type-D asteroids or fragments that interfused after a planetesimal collision with Mars. In terms of mission concepts, Phobos has also been considered as a natural space station that can be utilized by future crewed Martian missions to monitor and control robotic assets on the surface of Mars. Several dedicated missions in the past, such as Soviet Phobos 1, Phobos 2, and Phobos Grunt, have never or partially been successful.[1)] The Japan Aerospace Exploration Agency (JAXA) is currently planning a robotic sample return mission known as the Martian Moons eXploration (MMX), scheduled for a 2024 launch.[2)] The goal of the MMX mission is to explain the moons' origin and provide insights into the evolution of Mars and other small bodies in the Solar system. The current mission plan of MMX involves an interplanetary phase followed by a Mars orbit insertion phase, a Phobos proximity phase, and surface operations to perform descent and landing operations.[2,3)]

The dynamical environment around Phobos is unique compared to other planetary systems.[4)] Therefore, a simple two-body approximation with Mars is not appropriate to describe the dynamics in the vicinity of Phobos. Indeed, the size of the Martian moon is enough to perturb two-body motion during the proximity phase and make spacecraft operations quite challenging. MMX envisions utilizing quasi-satellite orbits (QSO) to characterize the dynamical environment of Phobos for adequate landing site selection and relatively safe spacecraft operations. QSOs are stable three-body orbits that demand lower orbit maintenance costs over long mission periods. For these reasons, QSOs have gained much attention over the past decade, becoming the subject of several studies found in literature.[5,6)]

This paper explores the bifurcations of QSOs and proposes novel transfer methodologies for transfers between relative QSOs in the proximity of Phobos. In particular, we utilize MMX baseline QSOs for mission design applications. During the proximity operations, the spacecraft will gradually descend from a high-altitude QSO towards a lower altitude orbit with suitable transfer techniques. It is also envisaged that MMX will fly on spatial retrograde orbits (hereafter referred to as 3D-QSOs) to assist with the scientific observations of Phobos and enable global coverage.[2)]

Despite studies on transfers between liberation point orbits and planet-centred orbits towards QSOs can be found in the literature,[7,8)] the problem of transferring between relative planar QSOs and planar to 3D-QSOs is still open to debate. Literature on transfers between relative planar QSOs includes the work of Russell,[9)] Ichinomiya et al.,[10)] and Pushparaj et al.[11,12)] Russell utilizes primer vector theory and low-thrust trajectories to maneuver satellites in the Jupiter-Europa and Earth-Moon systems. Ichinomiya et al.[10)] applied Lam's and Whiffen's approach to design transfers between planar QSOs in the Mars-Phobos CRTBP.[13)] This work presents an improved approach to this methodology by considering the Circular Hill Problem with ellipsoidal secondary and developing a transfer methodology via multi-revolution in-plane bifurcations of planar QSOs. We also consider vertical QSO bifurcations to design 3D-QSOs and assess their feasibility as staging orbits between high-altitude and low-altitude trajectories around Phobos. The advantages of

our approach are two-fold: 1) MMX mission intends to insert the spacecraft into an out-of-plane 3D-QSO in the mid-altitude region for comprehensive coverage of Phobos' high latitude regions. 2) 3D-QSOs can be mildly unstable, thus enabling the exploitation of stable and unstable manifolds to implement cheap transfer opportunities near the Martian moon.

We first calculate families of 3D QSOs that bifurcate from the planar and stable family using principles of dynamical systems theory. In-plane and Out-of plane bifurcations of periodic orbits were first studied by Robin and Markellos.[14] Later, Lara et al. used similar bifurcation methods to explore distant stability regions around Europa.[15] Vaquero and Howell[16] designed 3D resonant orbits bifurcating from planar resonant periodic families in the Sun-Earth CRTBP. Oshima and Yanao[17] applied the same bifurcation theory to calculate spatial QSOs and study their application in the bi-circular four-body problem of Sun-Earth-Moon system. More recently, Chen et al.[18] studied the effective stability of bifurcated 3D-QSOs for Phobos exploration. Transfers between planar and spatial QSOs were only studied by Canalias et al.,[19] whereby single impulsive maneuvers were implemented in order to insert from mid-altitude QSOs into their spatial and out-of-plane counterpart. Differently from previous studies, we thereby propose transfer methodologies that utilizes the bifurcated families of QSOs and their associated invariant manifolds to design in-plane and out-of-plane transfer trajectories connecting planar and stable QSOs. Considering the number of candidate solutions, we have also implemented a simple station-keeping strategy to rank 3D-QSOs and aid MMX mission designers in selecting the best possible candidate for proximity operations and global coverage.

2. Background

The general problem of satellite and particle dynamics about a tri-axial ellipsoid with constant density model is considered. The tri-axial ellipsoidal model of Phobos can be framed by specifying the physical parameters of the smaller body as follows. The largest semi-major axis constantly points along the x-axis, intermediate semi-major axis along the y-axis, and smallest semi-major axis along the z-axis. It is assumed that Phobos orbits around Mars in a tidal-locked configuration. As a result, the tri-axial ellipsoid representing the surface of the Martian moon does not rotate with respect to the Mars-Phobos synodic reference frame.

2.1. Model Specification and Gravitational Potential

The irregular gravity field of Phobos can be approximated using an ellipsoidal model with three major axes: α, β, and γ. Assuming constant density σ_P, the gravitational parameter of Phobos is computed as[20,21]

$$\mu_P = \frac{4\pi}{3} G \sigma_P \alpha\beta\gamma. \tag{1}$$

where G, is the gravitational constant $6.674 \times 10^{-8} cm^3 g^{-1} s^{-2}$ and $\frac{4\pi}{3}\alpha\beta\gamma$ is the volume of the ellipsoid. The gravitational potential of a constant density tri-axial ellipsoidal Phobos model at a point x, y, z, is given by

$$\mathcal{U}(x,y,z) = -\mu_P \frac{3}{4} \int_0^\infty \phi(x,y,z,u) \frac{dl}{\Delta(l+\Lambda)}, \tag{2}$$

where

$$\phi(x,y,z,l+\Lambda) = \frac{x^2}{\alpha^2+l+\Lambda} + \frac{y^2}{\beta^2+l+\Lambda} + \frac{z^2}{\gamma^2+l+\Lambda} - 1, \tag{3}$$

$$\Delta(l+\Lambda) = \sqrt{(\alpha^2+l+\Lambda)(\beta^2+l+\Lambda)(\gamma^2+l+\Lambda)}. \tag{4}$$

μ_P is the gravitational parameter of Phobos from the Eq.(1), whereas Λ is defined as either to be zero or the real positive root of $\phi(x,y,z,l+\Lambda) = 0$, depending on whether the gravitational attraction of Phobos is computed internally or externally of the body. The physical properties of Phobos are provided in.[22]

2.2. Equations of Motion

Since the gravitational parameter of Phobos is significantly smaller than the gravitational parameter of Mars and the relative distance between the spacecraft and Phobos is significantly smaller than the distance between Mars and its moons, the differential equations governing the motion of mass particles around Phobos can be well approximated via the Hill approximation of the Circular Restricted Three-Body Problem (CRTBP).[21,23] The Hill Problem's (HP) equations of motion are defined in a rotating reference frame located at the barycenter of the secondary.

$$\begin{cases} \ddot{x} - 2\dot{y} &= g_x + 3\,x, \\ \ddot{y} + 2\dot{x} &= g_y, \\ \ddot{z} &= g_z - z. \end{cases} \tag{5}$$

Here, $\vec{G_a} = [g_x, g_y, g_z]^T$ is the normalized acceleration due to an attracting ellipsoidal mass and it is given by

$$g_x = -\frac{3}{2}\mu_P x \int_0^\infty \left(\frac{1}{\alpha^2+l+\Lambda}\right) \frac{dl}{\Delta(l+\Lambda)}, \tag{6}$$

$$g_y = -\frac{3}{2}\mu_P y \int_0^\infty \left(\frac{1}{\beta^2+l+\Lambda}\right) \frac{dl}{\Delta(l+\Lambda)}, \tag{7}$$

$$g_z = -\frac{3}{2}\mu_P z \int_0^\infty \left(\frac{1}{\gamma^2+l+\Lambda}\right) \frac{dl}{\Delta(l+\Lambda)}. \tag{8}$$

Equations (2) and (6-8) are elliptic integrals which can be rapidly approximated using numerical procedures.[24] It is also worth noting that the equations of motion Eq.(5) admit an integral of motion known in the literature as the Jacobi integral and expressed as

$$C = \mathcal{W}(r) - \frac{1}{2}(\dot{x}^2 + \dot{y}^2 + \dot{z}^2), \tag{9}$$

where $\mathcal{W}(r) = \frac{1}{2}(3\,x^2 - z^2) + \mathcal{U}(r)$ is the effective potential of the system, and $\mathcal{U}(r)$ is the normalized acceleration due to an attracting ellipsoidal mass. Bifurcation analysis and key dynamic properties of distant retrograde orbits or quasi-satellite orbits (QSO) will be reviewed in the next section.

3. Bifurcated Quasi-Satellite Orbits

In this research, Phobos is assumed to move around Mars in a circular orbit with semi-major axis $a_P = 9377$ km. If we momentarily neglect its gravitational attraction, a spacecraft on an eccentric orbit with the same semi-major axis would remain in the vicinity of the Martian moon and describe purely periodic orbits with respect to the co-rotating frame of the planetary satellite. More specifically, spacecraft would describe 2:1 ellipses centered on Phobos and with period equal to its orbital period around Mars (7.66 hrs) as prescribed by the analytical solution of the Hill-Clohessy-Wiltshire (HCW) equations.[25)]

If we now consider the gravitational attraction of Phobos, the closer spacecraft to the surface of the Martian moon, the higher the gravitational influence of the planetary satellite on the relative trajectory of the spacecraft. Because of this perturbation, lower altitude QSOs are usually computed via differential corrector techniques that search for purely periodic orbits while migrating inwards from high-altitude 2:1 ellipses that are less affected by the gravity of the planetary satellite.

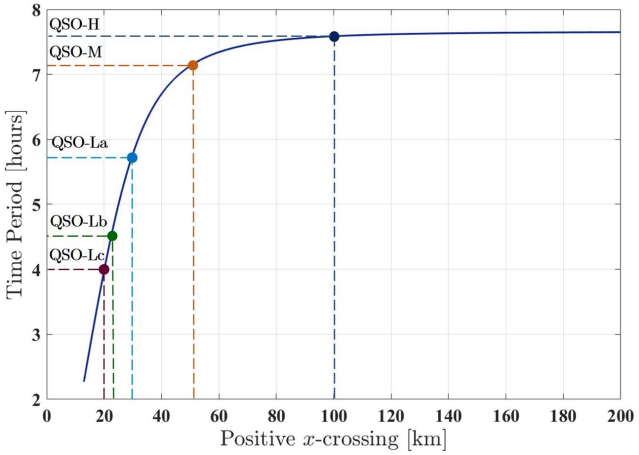

Fig. 1. Time Period vs positive x-axis crossing of the QSO family branch.

In this research, we have utilized pseudo-arclength continuation method of Mittelmann[26)]and shooting methods for calculating families of QSO as shown in the Fig.1. The current mission design of MMX envisages the utilization of different altitude planar QSOs in order to characterize the gravitational field before landing on Phobos. Key features of these baseline trajectories are tabulated in Table 1.[27)]

Table 1. MMX Candidate QSO.

Name	$x \times y$ (km)	$\dot{x} \times \dot{y}$ (m/s)	T (hrs)	C (−)
QSO-H	100×198.47	45.74×22.95	7.59	−8.78
QSO-M	50×94.41	23.41×12.04	7.13	−2.20
QSO-La	30×48.83	15.31×8.68	5.76	−0.78
QSO-Lb	22×30.81	12.79×8.25	4.40	−0.37
QSO-Lc	20×26.69	12.31×8.31	3.97	−0.27

3.1. Stability and Bifurcation analysis

The QSO family branch obtained through the pseudo-arclength continuation method[29)] is shown in Fig.2 with variations due to dynamical models. The bold line represents the QSO family in the ellipsoidal gravity model, and the dotted line represents the QSO family in HP point mass model, respectively. Fig.2 also illustrates the stability indices of the QSO family branch computed from Eq.(10).[28)]

$$b_j \equiv \lambda_j + \frac{1}{\lambda_j}, \quad j = 1, 2, \tag{10}$$

where λ_j and $1/\lambda_j$ are j^{th} reciprocal eigenvalues pairs of monodromy matrix, M.

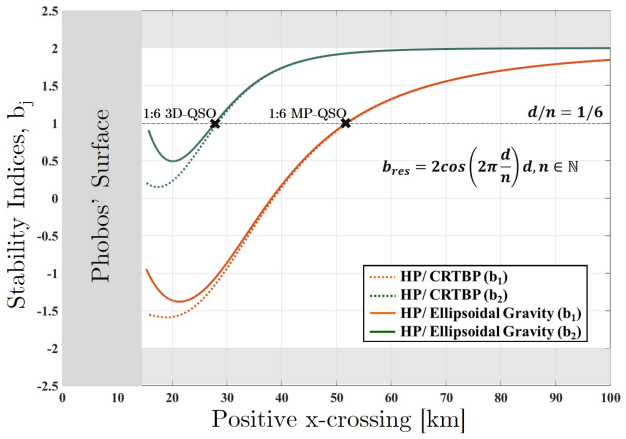

Fig. 2. Stability indices of planar QSO families. ($-2 < b_j < 2$ indicates periodic orbits are linearly stable)

As shown by the linear analysis, QSOs are linearly stable. We bifurcate from the planar QSO family using their stability indices as indicated in Eq.(11),

$$b_{Res} = 2\cos 2\pi\frac{d}{n}, \quad d, n \in N \tag{11}$$

where d and n are integer numbers.[14)] Note that the integer 'd' indicates a near-commensurability of period between the orbit at the point of bifurcation and the rotation of the coordinate system,[15)] whereas 'n' denotes the multiplicity of a periodic orbit, i.e., the number of revolutions around Phobos. Following Robin and Markellos[14)] and Lara et al.,[15)] families of multi-revolution periodic orbits can be found near stable QSOs when b_{Res} reaches any resonant value (d/n). Bifurcation points are detected using a bisection method on the curves of Fig. 2.

Let x_0^* and T^* be the initial state and orbital period of the bifurcation point. Once a positive x-axis crossing has been obtained, its corresponding QSO orbit is calculated leading to an accurate estimate of x_0^* and T^*. In addition, the monodromy matrix of the newly found QSO is multiplied for n times and diagonalized to approximate the direction of the researched $d:n$ bifurcated QSO family tangent. We consider $\tilde{Z}_0^* = \tilde{x}_0', \tilde{T}'^T$ be the family tangent of the bifurcated QSO family, where $\tilde{x}_0', \tilde{T}'^T$ are unit tangential state vector and propagation time to the solution curve at $Z_0^* = x_0^*, T^{*T}$ as shown in Fig. 3. This bifurcation analysis reveals that there are two families of QSOs emanating from each bifurcation point (*pitchfork* bifurcation). These two branches will be referred to as "symmetric" and "asymmetric" bifurcated QSOs depending on whether the radial velocity $(\dot{x}_0)$ of the predicted initial point, namely $x_0 = x_0^* \pm \varepsilon \tilde{x}_0'$, is equal or not to zero. To enforce the "symmetric" condition, we add

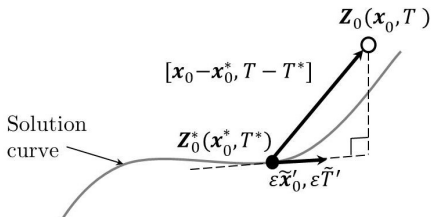

Fig. 3. Schematic of Pseudo-arclength continuation.

an additional constraint on the initial radial velocity of the bifurcated QSO and run a pseudo-arclength continuation procedure[26] that generates bifurcated in-plane QSO, and $z \neq 0$ and $\dot{z} = 0$ for bifurcated out-of-plane family branches from the initial conditions from Eq. (12) and family tangent $\tilde{Z}_0^*$.

$$\begin{cases} x_0 &= x_0^* \pm \varepsilon\, \tilde{x}_0', \\ T &= n\,T^* \pm \varepsilon\, \tilde{T}', \end{cases} \tag{12}$$

The variable ε is a small parameter, we used $\varepsilon = 10^{-4}$, whose magnitude can be adjusted throughout the continuation process to control the number of family members being computed.

Periodic orbits bifurcating via in-plane perturbations are referred to as swing QSOs or Multiple revolution Periodic QSOs (MP-QSOs), whereas the members bifurcating from out-of-plane perturbations are Spatial QSOs or 3D-QSOs.

4. Phobos Proximity Phase of MMX

This section introduces two transfer methodologies utilizing the bifurcated families of QSOs to explore the Martian moon, Phobos. The current mission plan of MMX envisages utilizing three QSOs at different altitudes, in order to gradually characterize the gravitational environment of Phobos and selecting the adequate landing sites. As the accuracy of the model of the gravity field of Phobos is improved, the spacecraft will descend to lower altitude QSO with increased reliability of the navigation system. In particular, MMX will be transferred from high to low-altitude QSOs (i.e., x = 100 km to 20 km) using the following sequences: QSO-H → QSO-M; QSO-M → QSO-La; QSO-La → QSO-Lb; QSO-Lb → QSO-Lc (refer Table 1 for the QSO specifications).

4.1. Out-of-plane transfer

In this subsection, we use 3D-QSOs computed from the out-of-plane bifurcations of the planar QSO family. T In this study, we propose and demonstrate an out-of-plane transfer methodology using the invariant manifolds of the 3D-QSOs(unstable). The invariant manifolds of a 3D-QSO are computed by perturbing the states along the direction of 3D-QSO's local eigenvectors. Stable and Unstable invariant manifolds originating from various regions along the unstable 3D QSOs are characterized using numerical computation on multiple nodes of the periodic 3D QSO.

To demonstrate the transfer methodology, we consider high- and low-altitude QSOs from the MMX baseline orbits, hereby referred to as QSO-H (A_x = 100 km) and QSO-La (A_x = 30 km), respectively. Firstly, a 3D-QSO-M (mid-altitude 3D-QSO) of desired A_z is identified (Fig.**??**). Secondly, we select 2000 equidistant nodes along the required unstable 3D-QSO-M and compute the local eigenvectors at each nodes to generate capture and escape trajectories. Finally, once stable and unstable manifolds are computed, we connect stable manifolds with QSO-H and unstable manifolds with QSO-L. This transfer procedure requires two transfer stages as illustrated in Fig.4.

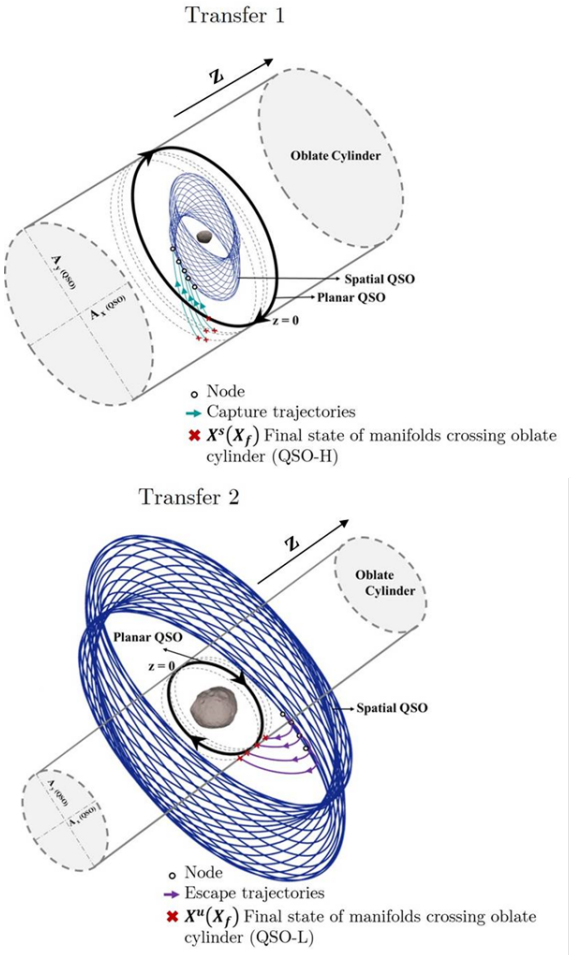

Fig. 4. Transfer stage illustration showing manifolds extraction from oblate cylinders passing through QSO-H and QSO-L.

The computed stable and unstable manifolds are discontinued during propagation while crossing an oblate cylinder passing through the QSO-H and QSO-L (See Fig.4). Capture trajectories are halted when they pass through QSO-H oblate cylinder and these final states are further refined to extract trajectories that intersect QSO-H at $|z| \leq 10^{-5}$. The refined trajectories allow us to calculate the ΔV^s and TOF^s from the departing planar QSO-H. Varying the number of nodes and changing the energy of the 3D-QSO provides better $z = 0$ crossing trajectories and lower ΔV^s. Similarly, escape trajectories from the same 3D-QSO-M are halted when they pass through the QSO-L oblate cylinder and the manifolds intersecting the QSO-L are recorded and extracted further to obtain ΔV^u and TOF^u at arriving planar QSO-L. Looking for feasible transfers between QSO-H and 3D-QSO-M, we investigated several cases of mid-altitude 3D-QSO families of different $A_z \in [70, 120]$ km and applied our transfer methodology.

4.1.1. Application to MMX

Combining the results of Transfer stage 1 and 2 could inform MMX mission designers on 3D-QSOs that would enable optimal transfers (in terms of either ΔV or TOF) between QSO-H

Table 2. MMX Injection Errors

Standard Deviation	Value	Unit
$\sigma_x, \sigma_y, \sigma_z$	100	m
$\sigma_{\dot{x}}, \sigma_{\dot{y}}, \sigma_{\dot{z}}$	3	cm/s

and QSO-L. However, such an analysis would not take into consideration the orbit maintenance costs required to operate the spacecraft at higher latitudes and collect precious images for the global coverage of Phobos. To better inform the selection of baseline 3D-QSOs, we have implemented an orbital maintenance approach that suppresses and eliminates the growth of the relative error along the unstable eigenvector of a 3D-QSO. Nakamiya and Kawakatsu[30] used this approach to estimate orbital maintenance of Halo orbits in the Sun-Earth system to eliminate unstable components under thrusting constraints.

Following the Hamiltonian nature of the system Eq.(5), the eigenvalues of the monodromy matrix, M must occur in reciprocal pairs. In the case of 3D-QSOs, the unstable eigenvalues (λ_1) cause neighboring trajectories to diverge from the desired periodic path. As a result, impulsive maneuvers should be implemented to nullify the exponential growth of the relative error. It is assumed that these initial errors are distributed according to zero-mean Gaussian distributions with standard deviations as reported in Table 2. Under the assumptions of our numerical simulation, it appears from the Table 3 that the orbital maintenance cost for the 1:27 3D-QSO with A_z = 120 km is the cheapest among the candidate orbits, with an estimated maximum correction maneuver v_{cm} cost of 0.584 m/s for 30 days. In contrast, the most expensive orbit turned out to be the 1:17 3D-QSO (A_z = 70 km) with a total v_{cm} cost of 0.937 m/s per month. All of the 3D-QSOs have orbital maintenance costs below 1 m/s per month, resulting in a plethora of valid candidate orbits for the global coverage of Phobos. This analysis suggests that the orbit maintenance costs of 3D-QSOs may play a minor role in driving the selection of an optimal staging orbit for transfers between high-altitude and low-altitude orbits around Phobos. Overall transfer cost including the station-keeping cost of mid-altitude QSOs are tabulated in Table 4. Note that '-' indicates no transfer connection (escape and capture trajectories of 3D-QSO) between QSO-H and La.

The minimum overall $\Delta V^t(\Delta V^s + \Delta V^u)$ and $TOF^t(TOF^s + TOF^u)$ transfer solution cases are shown in Fig.5 and 6, respectively. By comparison with our previous investigation where only planar transfers had been considered, we conclude that 17 m/s of additional ΔV would be required for the MMX spacecraft to be inserted into a mid-altitude 3D-QSO and enable the detailed observations of the high-latitude regions of Phobos (Table 5).

Table 3. Orbital maintenance cost of 3D-QSO-M for 30 days

	A_z = 70km	A_z = 80km	A_z = 90km	A_z = 100km	A_z = 110km	A_z = 120km
3D-QSO type	v_{cm} (m/s)	v_{cm} (m/s)	v_{cm} (m/s)	v_{cm} (m/s)	v_{cm} (m/s)	v_{cm} (m/s)
1:17	0.9376	0.9320	0.9283	0.9249	0.9219	0.9190
1:18	0.8860	0.8827	0.8798	0.8773	0.8750	0.8729
1:19	0.8395	0.8371	0.8349	0.8329	0.8311	0.8295
1:20	0.7972	0.7954	0.7936	0.7921	0.7906	0.7869
1:21	0.7586	0.7572	0.7558	0.7546	0.7534	0.7522
1:22	0.7235	0.7224	0.7212	0.7202	0.7191	0.7182
1:23	0.6913	0.6904	0.6895	0.6886	0.6877	0.6869
1:24	0.6617	0.6611	0.6600	0.6595	0.6588	0.6581
1:25	-	0.6341	0.6334	0.6327	0.6322	0.6314
1:26	0.6094	0.6090	0.6086	0.6086	0.6079	0.6068
1:27	0.5862	0.5859	0.5856	0.5850	0.5845	0.5840

Table 4. Overall transfer and station-keeping cost of mid-altitude 3D-QSOs.

	A_z = 70km	A_z = 80km	A_z = 90km	A_z = 100km	A_z = 110km	A_z = 120km
3D-QSO type	$\Delta V^t + v_{cm}$ (m/s)	$\Delta V^t + v_{cm}$ (m/s)	$\Delta V^t + v_{cm}$ (m/s)	$\Delta V^t + v_{cm}$ (m/s)	$\Delta V^t + v_{cm}$ (m/s)	$\Delta V^t + v_{cm}$ (m/s)
1:17	37.9737	45.6521	48.3913	55.5928	56.1084	64.1348
1:18	-	43.0563	47.1362	51.3869	-	-
1:19	-	44.6213	46.1121	54.4268	58.2922	62.4881
1:20	-	-	-	49.7909	57.7606	57.7867
1:21	-	44.7911	46.0979	50.3316	54.7476	62.0658
1:22	-	-	-	-	55.5314	58.0145
1:23	-	-	-	50.2637	54.0058	59.1082
1:24	-	-	-	-	54.2276	58.5609
1:25	-	-	-	-	54.6675	58.8815
1:26	-	-	-	-	55.2409	57.0393
1:27	-	-	-	-	-	60.0596

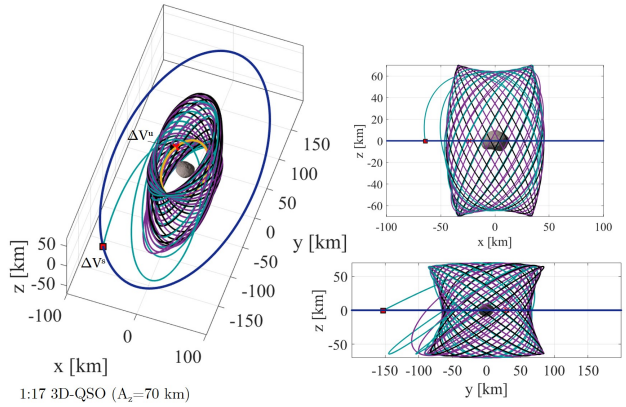

Fig. 5. Min ΔV^t transfer between QSO-H to QSO-L via 3D-QSO-M. [ΔV^t= 37.04 m/s; TOF^t= 9.47 days; v_{cm}=0.93 m/s]

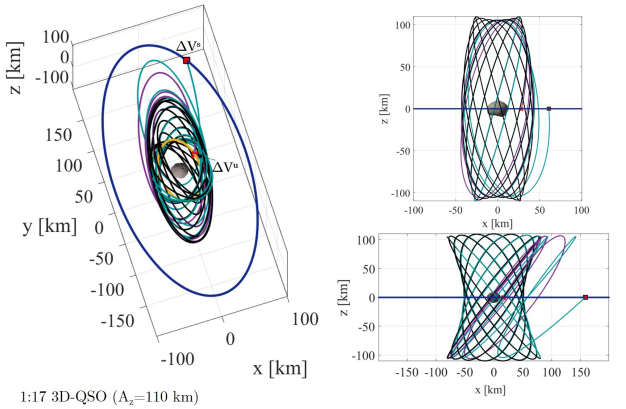

Fig. 6. Min TOF^t transfer between QSO-H to QSO-L via 3D-QSO-M. [ΔV^t= 55.19 m/s; TOF^t= 4.70 days; v_{cm}=0.92 m/s]

Table 5. Transfer cost for high-latitude coverage with 3D-QSOs

Transfer stage	Transfers via MP-QSOs min ΔV_{total}	Transfers via 3D-QSOs min ΔV_{total}	Difference min ΔV_{total}
QSO-H → QSO-La	21 m/s	37.97 m/s	16.97 m/s

5. Summary and Conclusions

The present study aimed at developing transfer trajectories connecting planar and spatial quasi-satellite orbits in the vicinity of Phobos. Firstly, we introduce an in-plane transfer method utilizing Multi-revolution Periodic QSOs (MP-QSOs) that bifurcate from planar solutions and register ΔV and time-of-flight values at multiple departing and arrival intersection points. By comparison with previous results, we find that the total transfer cost between the MMX baseline QSOs may be minimized by using MP-QSO families that intersect the departing and arrival orbits almost tangentially and with the highest possible value of the Jacobi integral. Such a conclusion contributes in sev-

eral ways to our understanding of the dynamical environment around Phobos, and provide a basis for the selection of transfer ΔV execution points. Secondly, we considered the out-of-plane bifurcated families of QSOs and propose an out-of-plane transfer strategy to insert the spacecraft into a 3D-QSO utilizing the stable and unstable manifolds emanating from unstable solutions. We later explored the feasibility of connecting high-altitude and low-altitude QSOs via cheap transfer opportunities. To design a transfer, we considered the intersection of capture and escape trajectories propagated from different locations along candidate 3D-QSOs with oblate cylinders passing through the baseline planar orbits of the MMX mission. This out-of-plane transfer technique provided us with a baseline to estimate the costs and time-of-flights associated with ballistic dynamics between high-altitude and low-altitude QSOs. To further narrow the design space of mid-altitude out-of-plane trajectories, a simple orbit maintenance strategy was implemented to nullify the growth of orbit injection errors along the unstable eigenvectors of candidate 3D-QSOs. As a result of our investigations, it was found that transfers from high-altitude to low-altitude regions around Phobos would be possible via intermediate 1:17 3D-QSOs that demands a minimum ΔV cost of 37.973 m/s and a minimum time of flight of less than 5 days. The transfer methodology and analysis presented in this paper can be extended for future missions that seek for low-ΔV transfer opportunities between stable retrograde orbits around Phobos or any small irregular planetary satellites in the solar system. In addition, the findings of this work could serve as initial guesses for transfer designs in higher-fidelity models of the Martian system. Future work will improve upon the identified transfer trajectories using appropriate optimization techniques that would allow us to simulate and account for more-realistic dynamics and engineering constraints.

References

1) Marov, M. Ya., Avduevsky, V. S.,Akim, E. L., Eneev, T. M., Kremnev, R. S., Kulikov, S. D., Pichkhadze, K. M., Popov, G. A., and Rogovsky, G. N.: Phobos-Grunt: Russian sample return mission, *Advances in Space Research*., **33**(2004), pp. 2276–2280.
2) Kawakatsu, Y., Kuramoto, K., Usui, T., Ikeda, H., Yoshikawa, K., Sawada, H., Ozaki, N., Imada, T., Otake, H., Maki, K., Otsuki, M., Muller, R., Zacny, K., Satoh, Y., Mary, S., Grebenstein, M., Tokaji, A., Yuying, L., Gonzalez-Franquesa, F., Pushparaj, N., and Chikazawa, T.: System Definition of Martian Moons eXploration (MMX), 71st International Astronautical Congress, The CyberSpace Edition, IAC-20,A3,4B,1,x59058, 2020.
3) Ikeda, H., Mitani, S., Mimasu, Y., Ono, G., Nigo, K., and Kawakatsu. Y.: Orbital Operations Strategy in the Vicinity of Phobos, 31st International Symposium on Space Technology and Science(ISTS), Matsuyama, Ehime, Japan, ISTS-2017-d-008, 2017.
4) Scheeres, D.J., Van Wal, S., Olikara, Z., and Baresi, N.: Dynamics in the Phobos environment, *Advances in Space Research.*, **63** (2019), pp. 476-495.
5) Hénon, M.:Vertical Stability of Periodic Orbits in the Restricted Problem II. Hill's Case, *Astronomy and Astrophysics*., **30** (1974), pp. 317–321.
6) Wiesel, W. E.: Stable orbits about the Martian moons, *Journal of Guidance, Control, and Dynamics*., **16** (1993), pp. 434–440.
7) Capdevila, L., Guzzetti, D., and Howell, K.C.: Various Transfer Options from Earth into Distant Retrograde Orbits in the Vicinity of the Moon, *Advances in the Astronautical Sciences.*, **152**(1) (2014), pp. 3659–3678.
8) Scott, C.J., and Spencer, D,B.: Transfers to Sticky Distant Retrograde Orbits, *Journal of Guidance, Control, and Dynamics.*, **33**(6) (2010), pp. 1940–1946.
9) Russell, R.P.: Primer Vector Theory Applied to Global Low-Thrust Trade Studies, *Journal of Guidance, Control, and Dynamics.*, **30**(2) (2007), pp. 460–472.
10) Ichinomiya, K., Baresi, N., Kawakatsu, Y., and Yanao, T.: Quasi-Satellite Orbit Transfers via Multi-Revolutional Periodic Orbits, AAS/AIAA Space Flight Mechanics Meeting, Hawaii, USA, AAS 19-422, 2019.
11) Pushparaj, N., Baresi, N., Ichinomiya, K., and Kawakatsu, Y.: Multi-Revolutional Periodic Orbit Transfers in the Ellipsoidal Gravity Field of Phobos, 32nd International Symposium on Space Technology and Science (ISTS), Fukui, Japan, ISTS-2019-d-022 2019.
12) Pushparaj, N., Baresi, N., Ichinomiya, K., and Kawakatsu, Y.: Transfers around Phobos via bifurcated retrograde orbits: Applications to Martian Moons eXploration mission, *Acta Astronautica.*, **181** (2021), pp. 70–80.
13) Lam, T., and Whiffen, G.J.:Exploration of Distant Retrograde Orbits Around Europa, AAS/AIAA Space Flight Mechanics Meeting, Copper Mountain, CO, USA, AAS 05-110, 2005.
14) Robin, I.A., and Markellos, V.V.: Numerical determination of three-dimensional periodic orbits generated from vertical self-resonant satellite orbits, *Celestial Mechanics.,* **21** (1980), pp. 395—434.
15) Lara, M., Russell, R., and Villac, B. F.: Classification of the Distant Stability Regions at Europa, *Journal of Guidance, Control, and Dynamics*., **30** (2007), pp. 409–418.
16) Vaquero, M., and Howell, K.C.: Design of transfer trajectories between resonant orbits in the Earth–Moon restricted problem, *Acta Astronautica.,* **94** (2014), pp. 302–317.
17) Oshima, K., and Yanao, T.: Spatial unstable periodic quasi-satellite orbits and their applications to spacecraft trajectories, *Celestial Mechanics and Dynamical Astronomy.,* **131**(23) (2019).
18) Chen, H., Canalias, E., Hestroffer, D., and Hou, X.: Effective Stability of Quasi-Satellite Orbits in the Spatial Problem for Phobos Exploration, *Journal of Guidance, Control, and Dynamics.,* **43**(12) (2020), pp. 2309–2320.
19) Canalias, E., Lorda, L., and Hekma, E.: Transfer between planar and three-dimensional Quasi Satellite Orbits in the vicinity of Phobos, AAS/AIAA Space Flight Mechanics Meeting, Hawaii, USA, AAS 19-248, 2019.
20) Wintner, A.: *The Analytical Foundations of Celestial Mechanics*, Princeton University Press, Princeton, NJ, 1947.
21) Scheeres, D.J.: *Orbital Motion in Strongly Perturbed Environments*, Springer-Verlag Berlin, 2012.
22) Willner, K., Shi, X., and Oberst, J.: Phobos' shape and topography models, *Planetary and Space Science.,* **102** (2014), pp 51–59.
23) MacMillan, W. D.: *The Theory of the Potential,* McGraw-Hill, New York, 1930.
24) Press, W.H., Teukolsky, S.A., Vetterling, W.T., and Flannery, B.P.: *Numerical Recipes: The Art of Scientific Computing*, Cambridge University Press, 3rd edition, 2007.
25) Clohessy, W.H., and Wiltshire, R.S.: Terminal guidance system for satellite rendezvous, *Journal of the Aerospace Sciences.,* **27** (1960), pp. 653-–658.
26) Mittelmann, H. D.: A Pseudo-Arclength Continuation Method for Nonlinear Eigenvalue Problems, *SIAM Journal on Numerical Analysis*., **23**(1986), pp. 1007–1016.
27) Baresi, N., and Kawakatsu, Y.: Quasi-periodic Motion around Phobos: Applications to the Martian Moons eXploration (MMX), 32nd International Symposium on Space Technology and Science (ISTS), Fukui, Japan, ISTS-2019-d-064, 2019.
28) Broucke, R.: Stability of periodic orbits in the elliptic, restricted three-body problem, *AIAA Journal.,* **7**(6) (1969), pp. 1003–1009.
29) Koon, W.S., Lo, M.W., Marsden, J.E., and Ross, S.D.: *Dynamical Systems, the Three-Body Problem and Space Mission Design*, Marsden Books, Wellington, 2011.
30) Nakamiya, M., and Kawakatsu, Y.: Maintenance of Halo Orbits Under the Thrusting Constraints, *Journal of Guidance, Control, and Dynamics.,* **35**(4) (2012), pp. 1224–1229.